ChemElectroChem

Research Article
doi.org/10.1002/celc.202400164

Chemistry Europe
European Chemical Societies Publishing

www.chemelectrochem.org

An Immersion Ultrasonic Testing-Based Research Platform for Studying Electroplating Kinetics

Yang Zirui[+],[a] Chen Yunda[+],[a] Fangxin Zou,*[a] and Frederic B. Cegla[b]

Electroplating is widely exploited in numerous application areas. Understanding the kinetics of electroplating, which is essentially a dynamic phenomenon, is crucial to making use of it appropriately in the real world. Currently, there exist a variety of research tools for studying electroplating kinetics, each with its own pros and cons. In this paper, we introduce a novel, immersion ultrasonic testing-based technique that carries out *in situ*, direct monitoring of the thickness increase of an electroplated layer. Through careful design and optimization of the measurement setup and the signal processing protocol, the measurement resolution of the technique was able to reach a sub-micron level. Via a number of demonstrative zinc plating experiments that were performed under different conditions, the measurement accuracy of the technique was thoroughly validated by a number of independent methods. All in all, the technique can become a promising alternative tool for studying the kinetics of different electroplating processes, supplementing the existing toolbox with the capability of providing a new class of information.

1. Introduction

Electroplating is utilized by a large number of industries for a wide range of purposes. The typical applications of electroplating include but are not limited to enhancing the visual appearances of objects, protecting objects against aggressive service conditions,[1–7] and fabricating new material structures and systems.[8–14] The functionality of electroplating is essentially enabled by the thin layer that it would deposit on a substrate.[15–25] With a view achieve greater process control over electroplating, researchers around the world have long been carrying out fundamental studies to understand the kinetics of electroplating.[26–30] As such, there exists high demand for research tools that can characterize the growth rates of electroplated layers.

The growth rate of an electroplated layer can be determined by using microscopic techniques, such as optical microscopy and scanning electron microscopy,[31–33] to gauge its end-state thickness. However, such approach, which is *ex situ* in nature, can only provide the average rate over a certain period of time, unable to reveal any intermediate rate changes. Electrochemical quartz crystal microbalances (EQCMs) were developed to resolve, in a *in situ* manner, the real-time growth rate of an electroplated layer.[34] In an electroplating experiment, an EQCM would be attached onto the substrate and the resonant frequency of the EQCM would be continuously recorded. By inputting, into the Sauerbrey equation, the resonant frequency shift of the EQCM, the mass change of the substrate, which ought to be contributed by the growth of an electroplated layer, would be obtained. Nevertheless, substrate mass is not the only factor that could influence the resonant frequency of an EQCM.[35] Therefore, the measurements obtained by EQCMs are sometimes prone to uncertainty.

Owing to some of its unique features such as low radiation level, high penetration depth and high sensitivity to morphological changes, ultrasonic testing (UT), in recent years, has emerged as an extremely popular approach for characterizing various aspects of materials.[36–42] In our previous work,[43] UT was effectively employed to monitor the growth rates of electroplated layers. To construct a monitoring setup, a piezoelectric transducer was permanently attached onto the non-working surface of the substrate. During an electroplating experiment, the piezoelectric transducer continuously transmitted ultrasonic waves across the thickness of the substrate and acquired the reflections off the working surface of the substrate. As an electroplated layer grew on the working surface of the substrate, the propagation path of the diagnostic signal became longer, and the time-of-arrival's (ToAs) of the reflections, larger. From the change in ToA of the reflections, it was possible to reconstruct, in real time, the thickness increase of the electroplated layer. The measurement resolution of the technique was shown to be as high as 10s nm. However, if the material of an electroplated layer is too different to that of the substrate, meaning that the ultrasonic wave velocities of the two phases would be too dissimilar, the measurement accuracy of the technique would be jeopardized, since the thickness reconstruction process would rely on the assumption that the diagnostic signal always travels at the ultrasonic wave velocity

[a] *Y. Zirui,[+] C. Yunda,[+] F. Zou*
Department of Aeronautical and Aviation Engineering, The Hong Kong Polytechnic University, Hung Hom, Kowloon, Hong Kong SAR, China
E-mail: frank.zou@polyu.edu.hk

[b] *F. B. Cegla*
Non-Destructive Evaluation Group, Department of Mechanical Engineering, Imperial College London, South Kensington Campus, London, SW7 2AZ, UK

[+] *These authors contributed equally to this work.*

Supporting information for this article is available on the WWW under https://doi.org/10.1002/celc.202400164

of the substrate, even when it is in the electroplated layer. Therefore, if a more robust technique was to be devised, the propagation path of the diagnostic signal in an experiment should embody only one medium.

In this work, we developed a new, immersion UT-based technique for monitoring the growth rates of electroplated layers. In a monitoring setup, a piezoelectric transducer was, in this case, positioned above the working surface of the substrate and at a certain distance away from it. In an electroplating experiment, the piezoelectric transducer was immersed in the electrolyte solution and transmitted ultrasonic compression waves that propagated towards, and reflected off, the working surface of the substrate. With the growth of an electroplated layer on the working surface of the substrate, the propagation path of the diagnostic signal shortened, hence causing the reflections to arrive earlier and earlier at the piezoelectric transducer. The performance of the technique was demonstrated through a series of zinc plating experiments that were conducted for different amounts of time or under different externally supplied electric currents. The measurement accuracy of the technique was assessed using both theoretical and experimental means, i.e., Faraday's law of electrolysis and optical profilometry. Since in an experiment the diagnostic signal propagates in only one medium, i.e., the electrolyte solution, the measurement accuracy of the technique is unaffected by mismatch between the material of an electroplated layer and that of the substrate.

Experimental

Immersion Ultrasonic Testing-Based Monitoring Setup

Figure 1(a) shows the hardware of the proposed ultrasonic technique for monitoring the growth rates of electroplated layers. To construct a monitoring setup, a custom-made reaction chamber that was fabricated by 3D printing was installed, using silicone rubber, on one of the two surfaces of the substrate. The reaction chamber served multiple purposes, including to hold in place the electrolyte solution and the anode that were used for each electroplating experiment, to affix a piezoelectric transducer with a concave lens (Guangzhou Doppler Electronic Technologies, China) at a distance of 5 cm from the working surface of the substrate, and to fasten a platinum resistance thermometer probe (SE012, Pico Technology, UK). The piezoelectric transducer and the platinum resistance thermometer probe were connected to an arbitrary waveform generator (AWG)/oscilloscope unit (Handyscope HS5, TiePie Engineering, Netherlands) and a platinum resistance data logger (PT104, Pico Technology, UK), respectively.

In an experiment, an electrolyte solution was filled into the reaction chamber, immersing a 30 cm^2 area on the working surface of the substrate, the anode, the piezoelectric transducer and the platinum resistance thermometer probe. A DC was applied across the substrate and the anode in order to drive the deposition of the anodic material onto the substrate. The piezoelectric transducer transmitted, at regular intervals, focused ultrasonic compression waves that each took the form of a Hanning-windowed 5-cycle sinusoidal toneburst with a central frequency of 2 MHz, and insonified a circular area with a diameter of 15 mm in the center of the substrate (see the Supporting Information for the procedure for

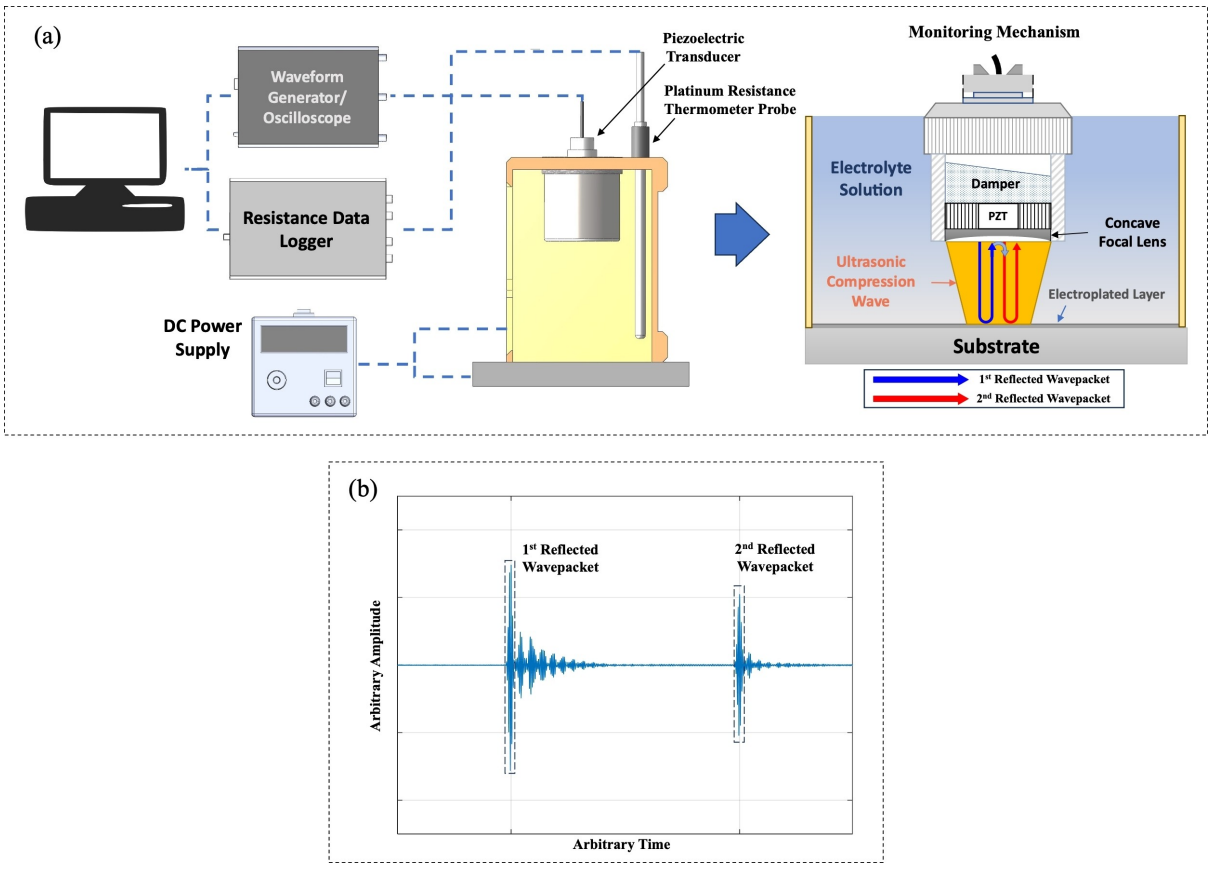

Figure 1. (a) A schematic diagram of the proposed ultrasonic technique for monitoring electroplating processes. (b) A typical reflection signal.

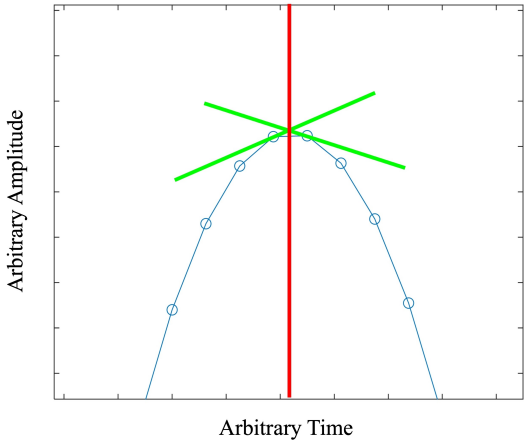

Figure 2. Gradient-based determination of the *true* ToA of a reflected wavepacket (blue: the *up-sampled auto-correlation* of the *averaged and de-noised* reflection signal, green: the gradients of the *up-sampled auto-correlation* at the two highest points in the proximity of the local maximum that corresponds to the reflected wavepacket of interest, red: the *true* location of the local maximum).

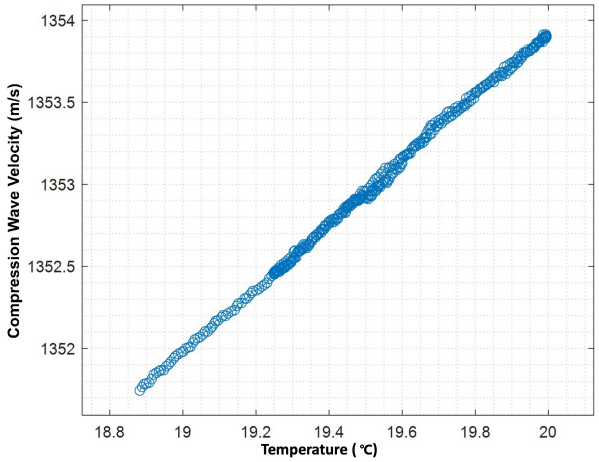

Figure 3. The compression wave velocity vs. temperature relationship of the electrolyte solution used.

Table 1. The details of the zinc plating experiments for evaluating the performance of the proposed ultrasonic monitoring technique.

	Experiment No.	Applied DC	Duration
Preliminary validation	1	0.2 A	60 min
	2	0.4 A	30 min
Parametric study – duration	3	0.4 A	50 min
	4		30 min
	5		4 min
Parametric study – applied DC	6	0.8 A	30 min
	7	0.6 A	
	8	0.4 A	
Parametric study – anode position	9	0.4 A	90 min
	10		
Parametric study – varying applied DC	11	10 min @ 0.2 A, 10 min @ 0.4 A, 10 min @ 0.8 A	

determining the insonification area of the piezoelectric transducer). Each of the waves "bounced" between the working surface of the substrate and the piezoelectric transducer for a few times before diminishing, resulting in a reflection signal that embodies multiple reflected wavepackets, as exemplified in Figure 1(b). Meanwhile, the thermometer probe continuously recorded the temperature of electrolyte solution. The thickness of the resultant electroplated layer at any moment in time was calculated by

$$Th(t) = D - \frac{(ToA_2 - ToA_1) \cdot c(T(t))}{2} \quad (1)$$

where $c(T(t))$ is the instantaneous temperature-dependent velocity of the compression wave transmitted (see Section 2.3 for the procedure for determining compression wave velocity vs. temperature relationships), ToA_1 and ToA_2 indicate the time-of-arrival's of the first and the second reflected wavepackets in the reflection signal acquired, and D (5 cm) is the initial distance between the piezoelectric transducer and the working surface of the substrate.

It is worth mentioning that the proposed ultrasonic monitoring technique has been standardized as far as possible in order to enable convenient construction of monitoring setups and to minimize the discrepancy between different experiments in terms of hardware. For instance, the slots on each reaction chamber, in which a piezoelectric transducer and a platinum resistance thermometer probe sat, were shaped precisely, according to the geometries of the two types of instruments, with a view to ensure that in any experiment, the positions of the piezoelectric transducer and platinum resistance thermometer probe used would not change.

Determination of Time-of-Arrival's of Reflected Wavepackets

The signal-to-noise ratio (SNR) of a reflection signal directly influences the measurement accuracy of the ToAs of the reflected wavepackets. In order to enhance the SNRs of reflection signals, three approaches were employed. For each thickness measurement point, 300 rounds of signal generation & acquisition were carried out, and the 300 consecutively acquired reflection signals were averaged over; the *averaged* reflection signal was de-noised by a 5th-order Butterworth bandpass filter with cut-off frequencies of 1.2 MHz and 2.8 MHz; the *averaged and de-noised* reflection signal was auto-correlated – the locations of the local maxima of the *auto-correlation* correspond to the ToAs of the reflected wavepackets in the *averaged and de-noised* reflection signal.

When a reflection signal, which is continuous in nature, is digitized, the *true* ToAs of the reflected wavepackets could very well be missed out on by the discrete sampling points. To minimize the effect of digitization on the measurement accuracy of the ToAs of reflected wavepackets, two tactics were adopted. For each thickness measurement point, the *auto-correlation* of the *averaged and de-noised* reflection signal was up-sampled from 200 MHz to 800 MHz, where 200 MHz is the highest sampling frequency of the AWG/oscilloscope unit used; as illustrated in Figure 2, the *up-sampled auto-correlation* had its gradients calculated at the two highest points in the proximity of each local maximum, and by linearly interpolating between these two gradients, the location of the zero-gradient point, which resembles more closely the *true* location of the local maximum, was be determined, resulting in a more accurate estimate of the ToA of the reflected wavepacket that the local maximum corresponds to.

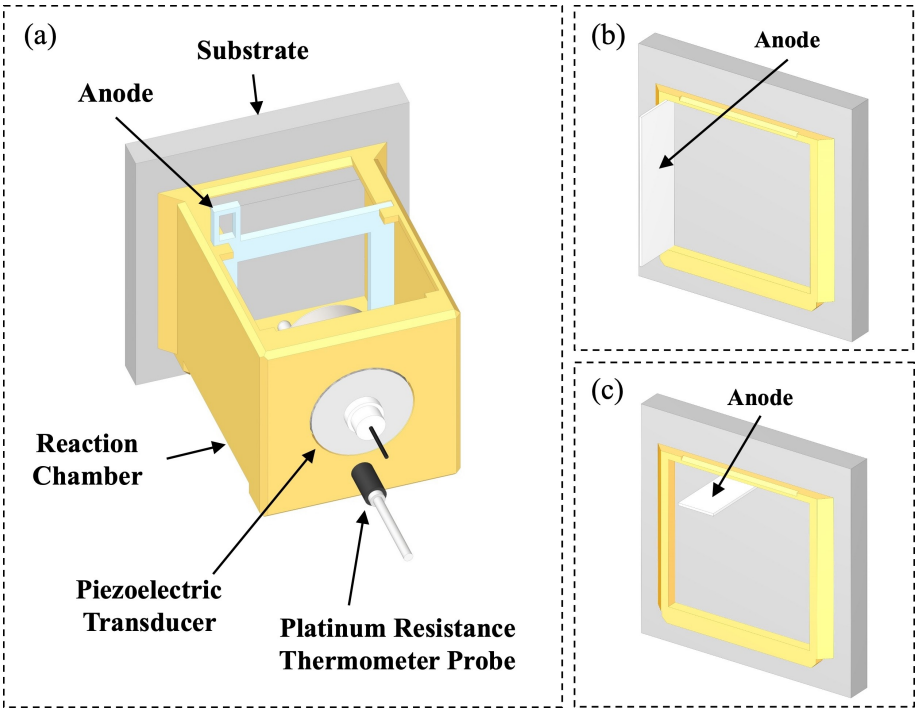

Figure 4. The anodes for (a) Experiments #1–8 and Experiment #11, (b) Experiment #9, and (c) Experiment #10.

Attainment of Compression Wave Velocities

The velocity of an ultrasonic wave varies with the temperature of the propagation medium. Nevertheless, during an electroplating process, the electrochemical reactions involved can actually cause the temperature of the electrolyte solution to fluctuate. In the case of the monitoring setups used in work (transducer-to-substate distance: 5 cm), a 1 °C variation in electrolyte solution temperature would lead to a 2 m/s variation in compression wave velocity and in turn a 750 μm uncertainty in thickness measurement. In order to minimize thickness measurement uncertainty, the exact compression wave velocity at any moment in time in an electroplating experiment would need to be attainable, and to achieve that, the compression wave velocity vs. temperature relationship of the electrolyte solution would need to be known in advance.

To determine the compression wave velocity vs. temperature relationship of an electrolyte solution, a monitoring setup that was filled with it was constructed and then exposed to room temperature for a certain amount of time. During the exposure, no electroplating was incurred and hence the thickness of the substrate remained unchanged; the piezoelectric transducer and the platinum resistance thermometer probe continuously carried out signal generation & acquisition and temperature measurement, respectively, just like what they would do in an actual electroplating experiment. For each measurement point, the ToAs of the first two reflected wavepackets in the reflection signal were extracted according to the procedure introduced in Section 2.2; the instantaneous compression wave velocity was calculated based on a modified version of equation (1), i.e., $c = 2 \cdot D/(ToA_2 - ToA_1)$. Finally, the compression wave velocities at all measurement points were plotted against the temperature variation recorded; the compression wave velocity vs. temperature relationship of the electrolyte solution was obtained via linear regression.

In an actual electroplating experiment, the compression wave velocity at each measurement point was attained based on both the instantaneous temperature of the electrolyte solution, and the pre-determined compression wave velocity vs. temperature relationship of the electrolyte solution.

2. Results and Discussion

2.1. Electrolyte Solution

The performance of the proposed ultrasonic monitoring technique was examined via a series of zinc plating experiments. The electrolyte solution used contains $ZnSO_4$ at 0.465 mol/L, $(NH_4)_2HC_6H_5O_7$ at 0.083 mol/L, and NH_4Cl at 0.5625 mol/L.[44] Among these ingredients, $(NH_4)_2HC_6H_5O_7$ serves as an optical brightener, and NH_4Cl, a complexing agent.

2.2. Compression Wave Velocity vs. Temperature Relationship

Figure 3 plots the compression wave velocities in the electrolyte solution used for this work at different temperatures. Expectedly, a highly linear trend is observed. Via linear regression, the compression wave velocity vs. temperature relationship of the electrolyte solution was found to be $c(T) = 1.9551T + 1314.8$.

2.3. Experimental Plan

Table 1 details the different zinc plating experiments that were designed to thoroughly evaluate the performance of the proposed ultrasonic monitoring technique. At first, the meas-

urement accuracy of the technique was preliminarily checked through two experiments which were conducted under different durations and applied DCs but ought to produce electroplated layers with the same thickness (Experiments #1 and #2). Then, further experiments were carried out under different durations, different applied DCs or different anode positions (Experiments #3–10) with a view to envision the robustness of the technique in real-life applications, especially when accurate theoretical predictions cannot be attained. At last, an experiment with a varying applied DC (Experiment #11) was performed in order to examine whether the technique could also capture intermediate changes in the kinetics of an electroplating process.

The anodes for the different zinc plating experiments are illustrated in Figure 4. For Experiments #1–8 and Experiment #11, n-shape anodes were purposely designed with a view to produce uniform electroplated layers, and meanwhile to avoid disturbance to the propagation of the diagnostic signal. For Experiments #9 and #10, off-centered strip-like anodes were utilized to induce a non-uniform distribution of current density over each substrate and hence cause the different points of each resultant electroplated layer to grow at different rates.

For each of the zinc plating experiments, the ultrasonic reconstruction was validated by both theoretical calculation and optical profilometry (see the Supporting Information for the procedure for making theoretical predictions based on Faraday's law of electrolysis, and that for obtaining optical measurements). Before each experiment, the working surface of the substrate was ground and polished using a series of sandpapers with increasing fineness (grit sizes: 80–4000), and then cleaned with deionized water and ethanol. After the experiment, the working surface of the substrate was flushed by deionized water.

2.4. Stability Analysis

For each of the zinc plating experiments, the stability of the monitoring setup, after it had been assembled, was assessed via an exposure test, during which no electroplating was incurred, and the thickness of the substrate, which in reality remained unchanged, was continuously monitored. As demonstrated in Figure 5(a), if the compression wave velocities at different measurement points were assumed to be the same, a thickness reconstruction that drifts with temperature would be obtained. On the other hand, if the compression wave velocity at each measurement point was independently calculated from the compression wave velocity vs. temperature relationship of the electrolyte solution and the instantaneous temperature of the electrolyte solution, the resultant thickness reconstruction would be much steadier. Figure 5(b) presents the standard deviations of the temperature-compensated thickness reconstructions obtained in all the exposure tests. In any case, a standard deviation of 100 s nm could be achieved, reflecting the high measurement resolution and high reproducibility of the proposed ultrasonic monitoring technique. The slight variation in standard deviation across the different tests is believed to be attributed to inevitable introduction of human errors to the assembly processes of the monitoring setups.

2.5. Preliminary Validation of Measurement Accuracy

Figure 6(a)–(b) displays the ultrasonic reconstructions of the growth processes of the electroplated layers produced in Experiments #1 and #2. While the intermediate thickness increases are benchmarked against the theoretical predictions made based on Faraday's law of electrolysis, the end-state thicknesses are compared to the optical measurements, the optical scans which were derived based on are presented in Figure 6(c)–(d). Generally speaking, the ultrasonic reconstructions match reasonably well with both the theoretical predictions and the optical measurements, confirming the measure-

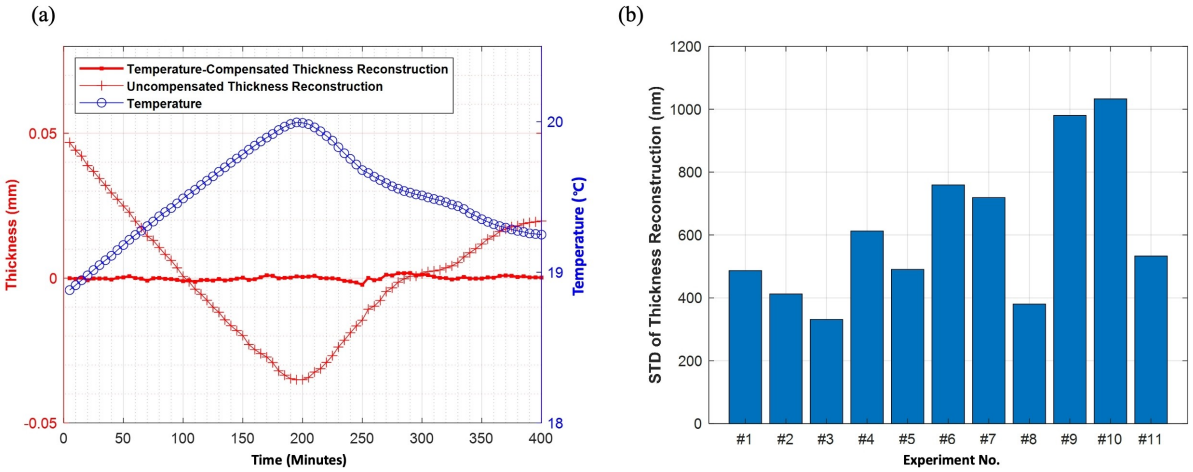

Figure 5. (a) The temperature variation occurred during, and the thickness reconstructions obtained in, the exposure test conducted before Experiment #1. (b) The standard deviations of the temperature-compensated thickness reconstructions obtained in all the exposure tests.

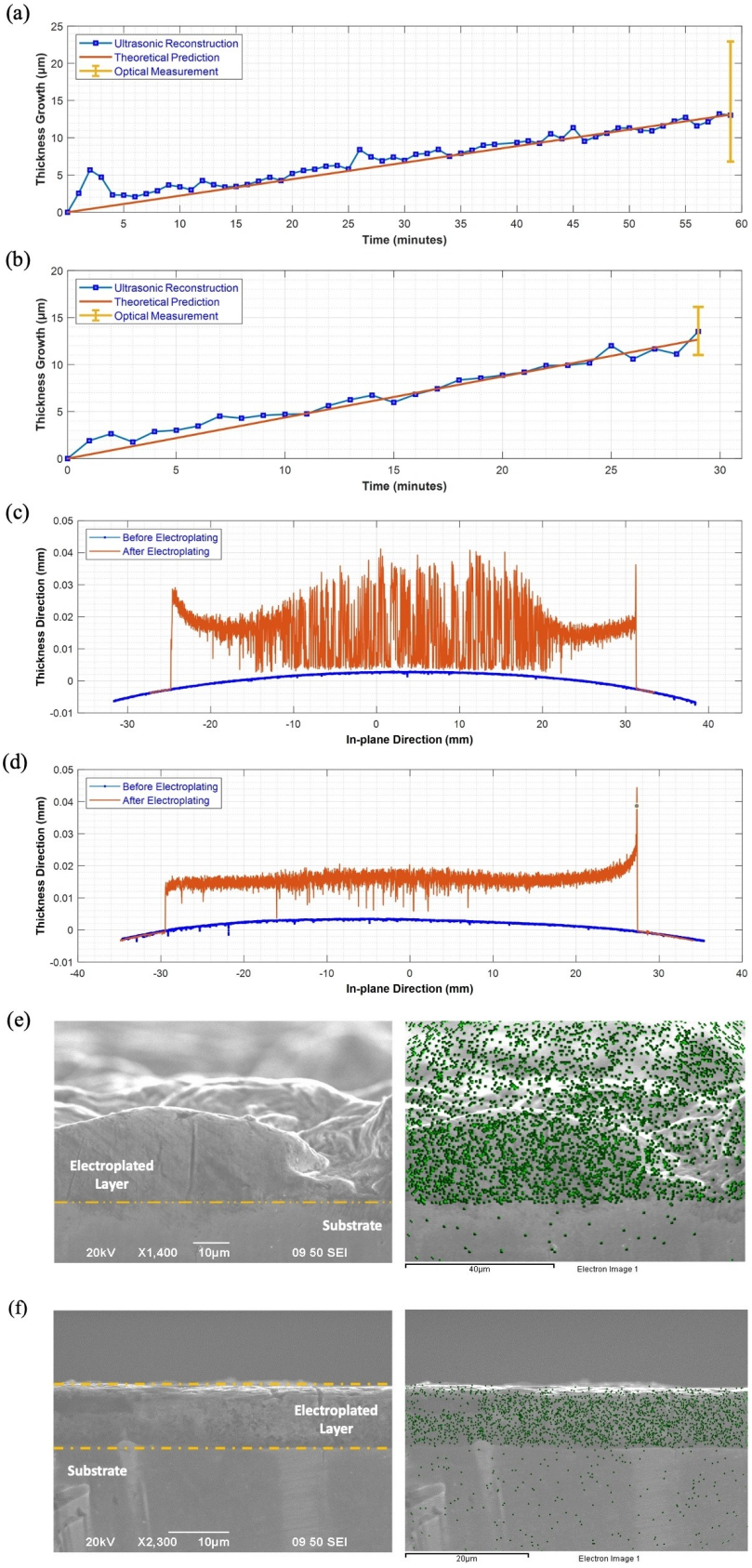

Figure 6. The ultrasonic reconstructions, theoretical predictions and end-state optical measurements of the thickness increases of the electroplated layers produced in (a) Experiment #1 and (b) Experiment #2 (error bar: ±1 standard deviation of all the pixel-based thickness increases). The optical scans of the centerlines of the electroplated layers produced in (c) Experiment #1 and (d) Experiment #2. The SEM-EDX results of the electroplated layers produced in (e) Experiment #1 and (f) Experiment #2 (green dots: zinc).

ment accuracy of the proposed ultrasonic monitoring technique. The fluctuations in the ultrasonically reconstructed thickness increases, which are often much more significant than the expected measurement uncertainty of the technique (standard deviation: 100 s nm, see Section 3.4), can be attributed to the repeated accumulation and dissipation of bubbles on the surfaces of the electroplated layers during the experiments (see Section 3.6 for a more detailed analysis). Furthermore, the high surface roughness of the electroplated layer produced in Experiment #1, which is reflected by the optical scan, is also evident through the SEM-EDX result presented in Figure 6(e)–(f) (see the Supporting Information for the procedure for conducting SEM-EDX analysis).

2.6. Parametric Studies

Three experiments were conducted under different durations but the same applied DC. From Figure 7(a)–(b), it can be seen that for either Experiment #3 or Experiment #4, the ultrasonic reconstruction agrees decently with the theoretical prediction and the optical measurement, further ascertaining that the proposed ultrasonic monitoring technique possesses a sufficiently high measurement accuracy. Experiment #5 was carried out with a view to comprehend the fluctuations in the ultrasonically reconstructed thickness increases of electroplated layers. As observed from Figure 7(c)–(d), the significant deviations of the ultrasonically reconstructed thicknesses from the theoretically predicted thicknesses, at the 2nd and the 3rd measurement points, were accompanied by the emergence of bubbles on the surface of the electroplated layer. Before the 4th measurement began, a dropper was inserted into the electrolyte solution to gently blow away the bubbles, and as a result, the ultrasonically reconstructed thickness at the 4th measurement point resembled much more closely the theoretically predicted thickness as well as the optically measured thickness.

Another set of three experiments were conducted, this time, under the same duration but different applied DCs. As demonstrated in Figure 8(a)–(c), the ultrasonic reconstructions are once again well validated by the theoretical predictions and the optical measurements. Thanks to the high measurement resolution of the proposed ultrasonic monitoring technique, the growth rates of the electroplated layers produced in these experiments, which ought to differ from each other, are clearly distinguishable. The relatively more intense fluctuation in the ultrasonically reconstructed thickness increase of the electroplated layer produced in Experiment #6 owes to the high applied DC of 0.8 A, which should

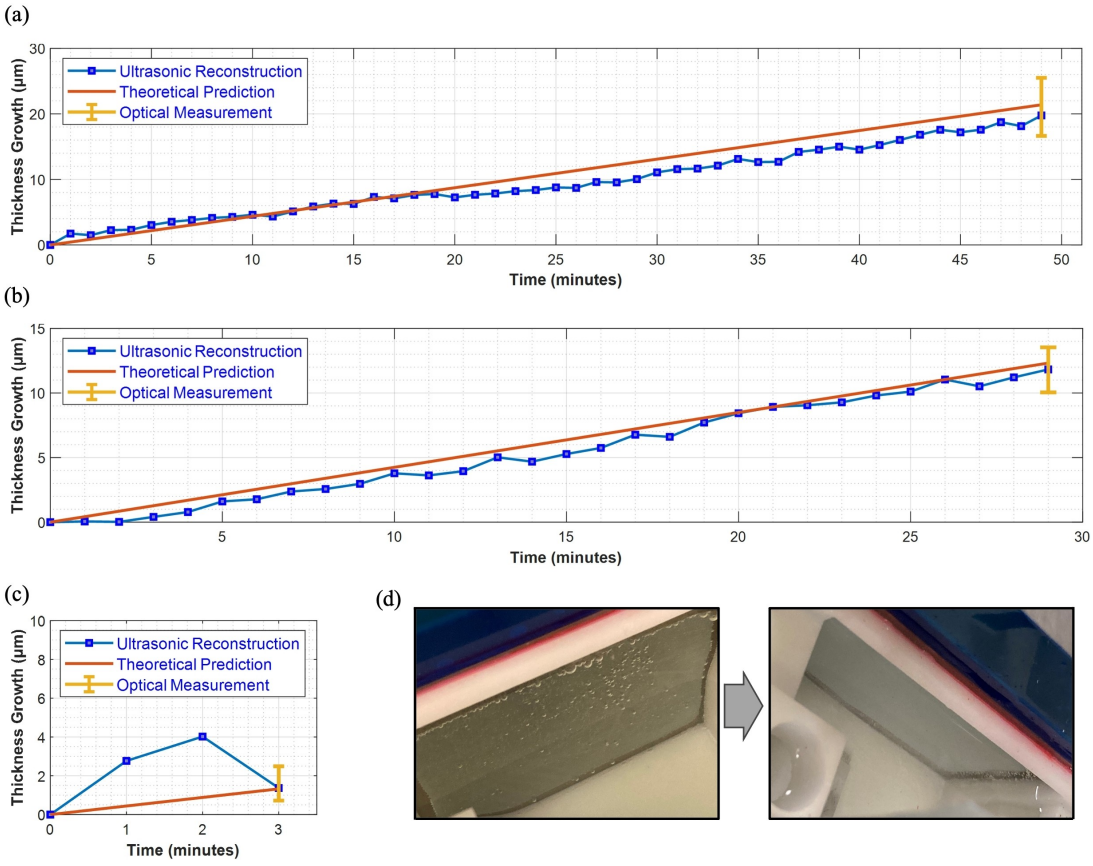

Figure 7. The ultrasonic reconstructions, theoretical predictions and end-state optical measurements of the thickness increases of the electroplated layers produced in (a) Experiment #3, (b) Experiment #4 and (c) Experiment #5 (error bar: ±1 standard deviation of all the pixel-based thickness increases; see Figure S3 in the Supporting Information for the optical scans). (d) The accumulation and dissipation of bubbles in Experiment #5.

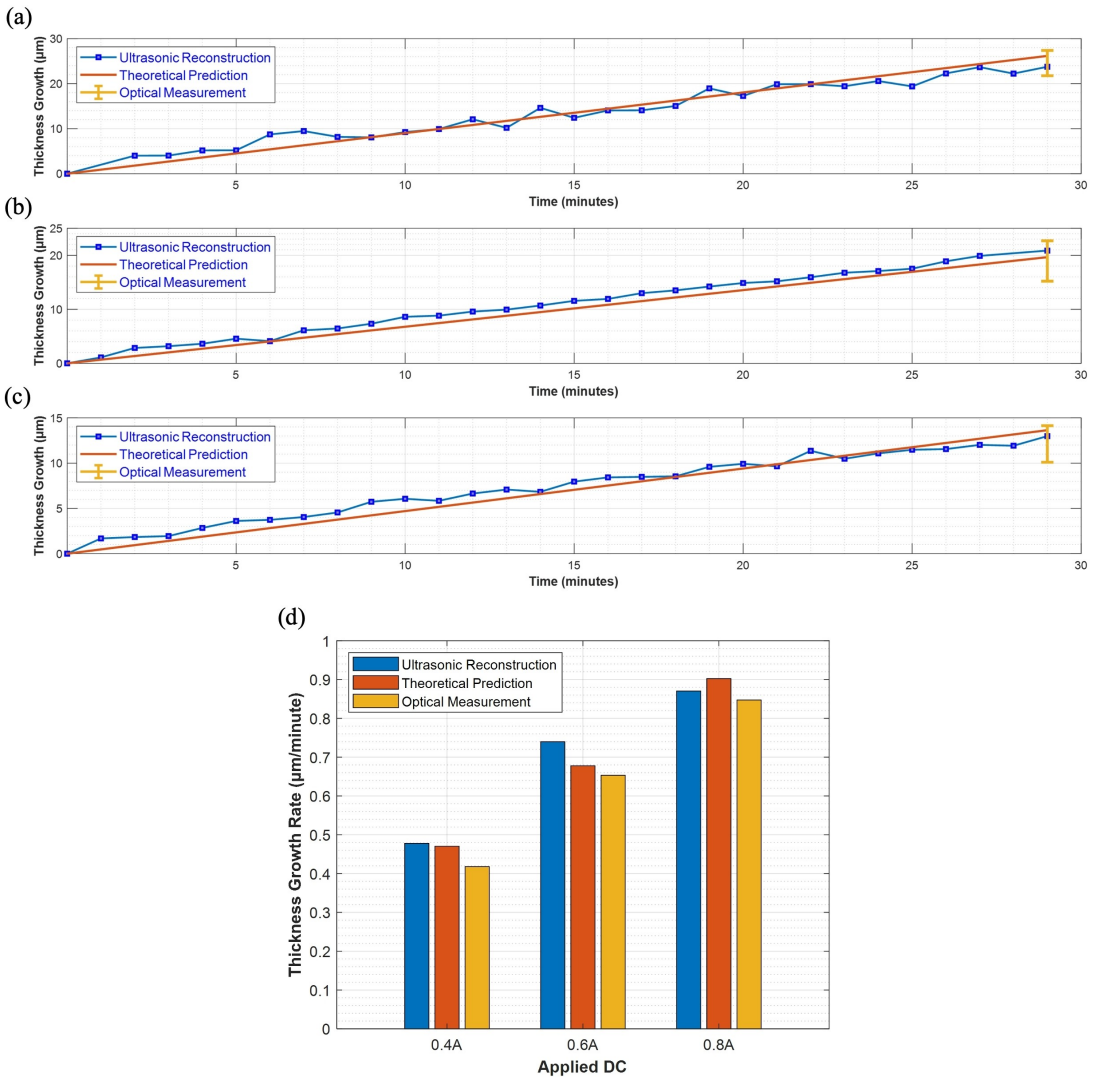

Figure 8. The ultrasonic reconstructions, theoretical predictions and end-state optical measurements of the thickness increases of the electroplated layers produced in (a) Experiment #6, (b) Experiment #7 and (c) Experiment #8 (error bar: ±1 standard deviation of all pixel-based thickness increases; see Figure S3 in the Supporting Information for the optical scans). (d) The growth rates of the electroplated layers, determined by the three different approaches.

induce more severe accumulation and dissipation of bubbles on the surface of the electroplated layer.

Figure 8(d) presents the ultrasonically reconstructed, theoretically predicted and optically measured growth rates of the electroplated layers produced in Experiments #6–8. While the ultrasonically reconstructed growth rates were obtained via linear regression, i.e., fitting a linear line to the ultrasonically reconstructed thicknesses of each electroplated layer, the optically measured growth rates were calculated by dividing the optically measured end-state thickness of each electroplated layer by the duration of the experiment. For any of the three electroplated layers, the ultrasonically reconstructed growth rate differs from neither the theoretically predicted growth rate nor the optically measured growth rate by more than 15%, proving the capability of the proposed ultrasonic monitoring technique to accurately quantify the growth rates of electroplated layers.

In Experiments #9 and #10, non-uniform electroplated layers were produced, as confirmed by optical scans presented in Figure 9(a)–(b). Based on the ultrasonic reconstructions and the optical measurements presented in Figure 9(c)–(d), it is ascertained that the electroplated layers produced in the two experiments grew at different rates at the insonification area of the piezoelectric transducer. Nevertheless, this difference in growth rate is not captured by the theoretical predictions which can only output the mean thickness increase of the entire electroplated layer on each substrate. Through these experiments, the value of the proposed ultrasonic monitoring technique in scenarios which are not readily predictable by theory, is clearly exemplified.

In Experiment #11, the applied DC was gradually increased in order to produce an electroplated layer that grows at different rates. As shown in Figure 10, the ultrasonic reconstruction was not only able to identify the end-state thickness of the electroplated layer, but also capable of capturing the

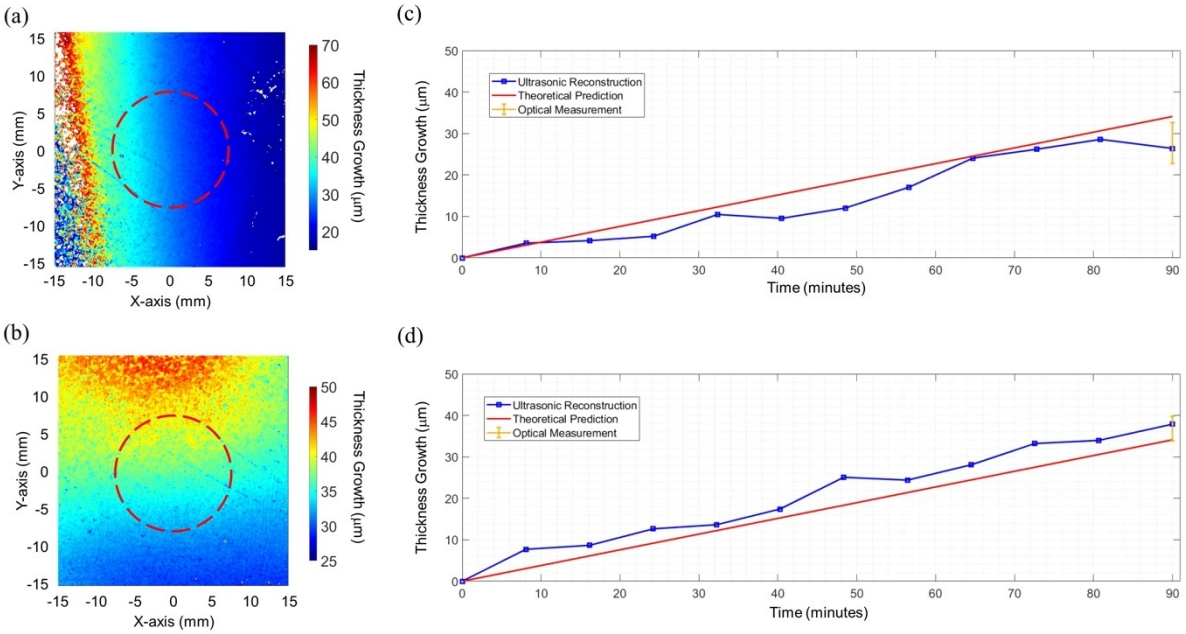

Figure 9. The 3D optical scans of the deposition areas of (a) Experiment #9 and (b) Experiment #10 (the red circles indicate the insonification area of the piezoelectric transducer). The ultrasonic reconstructions, theoretical predictions and optical measurements of the thickness increases of the electroplated layers produced in (c) Experiment #9 and (d) Experiment #10 (the ultrasonic reconstructions and optical measurements reflect the information of the electroplated layers within the insonification area of the piezoelectric transducer).

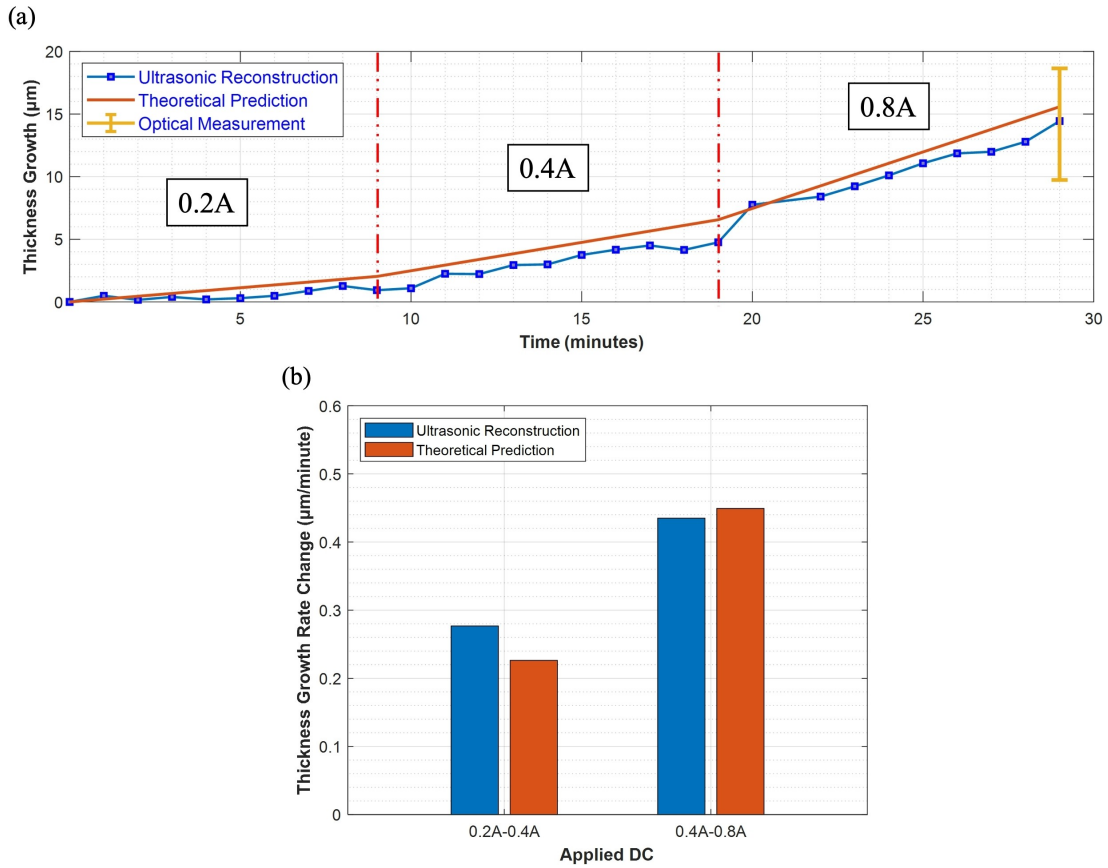

Figure 10. (a) The ultrasonic reconstructions, theoretical predictions and optical measurements of the thickness increases of the electroplated layer produced in Experiment #11 (see Figure S3 in the Supporting Information for the optical scans). (b) The changes in the growth rate of the electroplated layer, calculated from the ultrasonic reconstruction and the theoretical prediction.

expected growth rate changes. The result demonstrates the serviceability of the proposed ultrasonic monitoring technique in more realistic electroplating processes, during which the growth process of an electroplated layer might not always follow a constant rate.

3. Conclusions

In this paper, we introduce an immersion UT-based research technique for studying electroplating kinetics. Compared with the existing methods, the proposed technique is *in situ* and monitors directly the thickness increases of electroplated layers. The measurement resolution of the technique was shown to be sub-micron, thanks to the carefully crafted measurement setup and signal processing protocol. The technique was applied to monitoring a series of zinc plating processes that took place under different conditions, and by benchmarking the ultrasonic reconstructions to independent theoretical predictions and optical measurements, it was demonstrated that the technique was not only able to accurately reconstruct the end-state thicknesses of electroplated layers, but also capable of promptly alerting intermediate changes in the growth rate of an electroplated layer. In summary, the proposed technique, which interrogates electroplating processes from a different perspective, has much potential to become an important new tool for studying electroplating kinetics.

From the working principle of the proposed technique, it is not difficult to deduce that the measurement resolution of the technique is directly related to how exact the temperatures of the propagation path of the diagnostic signal can be gauged and how accurate the ToAs of reflected wavepackets can be determined. To minimize the effect of the potential existence of a temperature gradient within an electrolyte solution, one could, at each thickness measurement point, gauge the temperatures of an electrolyte solution at multiple locations by inserting multiple thermometer probes into the reaction chamber, and evaluate the mean temperature of the different locations or even establish the temperature gradient along the propagation path of the diagnostic signal. On the other hand, the accuracy of determination of the ToAs of reflected wavepackets will certainly benefit from better oscilloscopes with higher sampling frequencies and lower noise floors, and more advanced signal processing techniques for de-noising and up-sampling digitized reflection signals.

Acknowledgements

This work is supported by the National Natural Science Foundation of China (Project No.: 52201089) and the Department of Science and Technology of Guangdong Province (Project No.: 2021A1515012130).

Conflict of Interests

The authors have no conflict of interest to declare.

Data Availability Statement

The data that support the findings of this study are available from the corresponding author upon reasonable request.

Keywords: Electrodeposition · zinc plating · ultrasonic testing · analytical methods · surface analysis

[1] K. Novotný, T. Vaculovič, M. Galiová, V. Otruba, V. Kanický, J. Kaiser, M. Liška, O. Samek, R. Malina, K. Páleníková, *Appl. Surf. Sci.* **2007**, *253*, 3834–3842.
[2] O. Oluwole, D. Oloruntoba, O. Awheme, *Corros. Eng. Sci. Technol.* **2008**, *43*, 320–323.
[3] O. Oluwole, D. Oloruntoba, O. Awheme, *Mater. Des.* **2008**, *29*, 1266–1274.
[4] M. Lebrini, G. Fontaine, L. Gengembre, M. Traisnel, O. Lerasle, N. Genet, *Corros. Sci.* **2009**, *51*, 1201–1206.
[5] H. Katayama, S. Kuroda, *Corros. Sci.* **2013**, *76*, 35–41.
[6] H.-H. Sheu, P.-C. Huang, L.-C. Tsai, K.-H. Hou, *Surf. Coat. Technol.* **2013**, *235*, 529–535.
[7] L. Fathyunes, *Journal of Materials Research and Technology* **2021**, *14*, 2345–2356.
[8] A. K. Ayal, A. K. Hashim, A. M. Mohammed, A. M. Farhan, A. M. Holi, Y.-C. Lim, *J. Electron. Mater.* **2021**, *50*, 5161–5167.
[9] N. Endo, N. Dezawa, Y. Komo, T. Maeda, *Int. J. Hydrogen Energy* **2021**, *46*, 32570–32576.
[10] Z. Lai, T. Zhao, Zhu, D. Liu, X. Liang, R. Sun, *ACS Appl. Electron. Mater.* **2021**, *3*, 3329–3337.
[11] Q. Liu, Y. Chen, J. Ma, X.-B. Xiong, X.-R. Zeng, H. Qian, *Surf. Coat. Technol.* **2021**, *421*, 127452.
[12] Q. Niu, F. Wang, *Microelectron. Eng.* **2021**, *247*, 111582.
[13] M. del Carmen Mejia, M. Graske, A. Winter, C. Baumer, M. Stich, C. Mattea, A. Ispas, N. A. Isaac, Schaaf, S. Stapf, *J. Electrochem. Soc.* **2023**, *170*, 072504.
[14] W. Moteki, Y. Norikawa, T. Nohira, *ECS Trans.* **2022**, *109*, 225.
[15] J. Luo, A. Flewitt, S. Spearing, N. Fleck, W. Milne, *Mater. Lett.* **2004**, *58*(17–18), 2306–2309.
[16] S. Cho, S. Kim, N.-E. Lee, H. Kim, Y. Nam, *Thin Solid Films* **2005**, *475*(1–2), 68–71.
[17] S. Cho, S. Kim, J. Lee, N.-E. Lee, *Microelectron. Eng.* **2005**, *77*, 116–124.
[18] Z. Zhang, W. Leng, Q. Cai, F. Cao, J. Zhang, *J. Electroanal. Chem.* **2005**, *578*, 357–367.
[19] J. Luo, M. Pritschow, A. Flewitt, S. Spearing, N. Fleck, W. Milne, *J. Electrochem. Soc.* **2006**, *153*, D155.
[20] S. Park, Y. J. Song, J.-H. Han, H. Boo, T. D. Chung, *Electrochim. Acta* **2010**, *55*, 2029–2035.
[21] C. Yu, Y. Yang, J. Chen, J. Xu, J. Chen, H. Lu, *Mater. Lett.* **2014**, *128*, 9–11.
[22] A. Mahapatro, S. K. Suggu, *Adv. Mater. Sci* **2018**, *3*, 1.
[23] D. S. Solovjev, I. A. Solovjeva, V. V. Konkina, Y. V. Litovka, *Materials Today, Proceedings* **2019**, *19*, 1895–1898.
[24] V. P. Nguyen, T. N. Dang, C. C. Le, D.-A. Wang, *J. Therm. Spray Technol.* **2020**, *29*, 1968–1981.
[25] W. Shen, H. Ding, J. Zhang, M. Zhong, S. Guo, *ChemElectroChem* **2021**, *8*, 3651–3657.
[26] Y. Xiang, T. Tsui, J. J. Vlassak, *J. Mater. Res.* **2006**, *21*, 1607–1618.
[27] A. T. Jennings, M. J. Burek, J. R. Greer, *Phys. Rev. Lett.* **2010**, *104*, 135503.
[28] C. Wang, J. Zhang, Yang, M. An, *Electrochim. Acta* **2013**, *92*, 356–364.
[29] S. M. Rosa-Ortiz, K.-K. Phan, N. Khattak, S. W. Thomas, A. Takshi, *J. Electroanal. Chem.* **2021**, *902*, 115796.
[30] N. T. Hai, M. Broekmann, *ChemElectroChem* **2015**, *2*, 1096–1099.
[31] A. Bakkar, V. Neubert, *Electrochem. Commun.* **2007**, *9*, 2428–2435.
[32] T. Byk, T. Gaevskaya, L. Tsybulskaya, *Surf. Coat. Technol.* **2008**, *202*, 5817–5823.
[33] Y. Z. Su, Y. C. Fu, Y. M. Wei, J. W. Yan, B. W. Mao, *ChemPhysChem* **2010**, *11*, 2764–78.

[34] A. R. Hillman, *J. Solid State Electrochem.* **2011**, *15*, 1647–1660.
[35] S. Chandra, *Comprehensive Inorganic Chemistry Vol. Ii.* 2006, New Age International.
[36] J. Rao, M. Ratassepp, D. Lisevych, M. Hamzah Caffoor, Z. Fan, *Sensors* **2017**, *17*, 2882.
[37] B. Lan, T. B. Britton, T.-S. Jun, W. Gan, M. Hofmann, F. P. Dunne, M. J. Lowe, *Acta Mater.* **2018**, *159*, 384–394.
[38] W. Choi, F. Shi, M. J. Lowe, E. A. Skelton, R. V. Craster, W. L. Daniels, *NDT&E Int.* **2018**, *98*, 27–36.
[39] F. Zou, *Data-Enabled Discovery and Applications* **2018**, *2*, 1–5.
[40] F. Zou, F. B. Cegla, *J. Electroanal. Chem.* **2018**, *812*, 115–121.
[41] F. Zou, F. B. Cegla, *Corrosion* **2018**, *74*, 372–382.
[42] X. Wang, M. Lin, J. Li, J. Tong, X. Huang, L. Liang, Z. Fan, Y. Liu, *Mechanical Systems and Signal Processing* **2022**, *169*, 108761.
[43] F. Zou, F. B. Cegla, *Electrochem. Commun.* **2017**, *82*, 134–138.
[44] J. Rushmere, *Acid zinc electroplating electrolyte, process and additive.* 1974, Google Patents.

Manuscript received: February 19, 2024
Version of record online: April 11, 2024